www.nature.com/bjc

British Journal of Cancer

ARTICLE

Cellular and Molecular Biology

HIF-1α stimulates the progression of oesophageal squamous cell carcinoma by activating the Wnt/*β-catenin* signalling pathway

Kang Tang[1], Takeshi Toyozumi[1]✉, Kentaro Murakami[1], Haruhito Sakata[1], Masayuki Kano[1], Satoshi Endo[1], Yasunori Matsumoto[1], Hiroshi Suito[1], Masahiko Takahashi[1], Nobufumi Sekino[1], Ryota Otsuka[1], Kazuya Kinoshita[1], Soichiro Hirasawa[1], Jie Hu[1], Masaya Uesato[1], Koichi Hayano[1] and Hisahiro Matsubara[1]

© The Author(s), under exclusive licence to Springer Nature Limited 2022

BACKGROUND: This study aimed to clarify the significance of the crosstalk between hypoxia-inducible factor-1α (HIF-1α) and the Wnt/β-catenin pathway in oesophageal squamous cell carcinoma (ESCC).
METHODS: The oncogenic role of HIF-1α in ESCC was investigated using in vitro and in vivo assays. The clinicopathological significance of HIF-1α, β-catenin and TCF4/TCF7L2 in ESCC were evaluated using quantitative real-time PCR and immunohistochemistry.
RESULTS: The expression level of HIF-1α, β-catenin, and TCF4/TCF7L2 in T.Tn and TE1 cell lines were elevated under hypoxia in vitro. HIF-1α knockdown suppressed proliferation, migration/invasion and epithelial–mesenchymal transition (EMT) progression, induced G0/G1 cell cycle arrest, promoted apoptosis and inhibited 5-fluorouracil chemoresistance in vitro. In vivo assays showed that HIF-1α is essential in maintaining tumour growth, angiogenesis, and 5-fluorouracil chemoresistance. Mechanically, we identified the complex between HIF-1α and β-catenin, HIF-1α can directly bind to the promoter region of TCF4/TCF7L2. The mRNA level of HIF-1α, β-catenin and TCF4/TCF7L2 were increased in ESCC tumour tissues compared to the corresponding non-tumour tissues. High levels of HIF-1α and TCF4/TCF7L2 expression were correlated with aggressive phenotypes and poor prognosis in ESCC patients.
CONCLUSIONS: HIF-1α serves as an oncogenic transcriptional factor in ESCC, probably by directly targeting TCF4/TCF7L2 and activating the Wnt/β-catenin pathway.

British Journal of Cancer (2022) 127:474–487; https://doi.org/10.1038/s41416-022-01825-3

INTRODUCTION

Oesophageal squamous cell carcinoma (ESCC) remains a challenging malignancy to treat, with a poor prognosis and an overall 5-year survival variability ranging from 15 to 25% [1, 2]. Reduced oxygen utilisation (hypoxia) is a common but fundamental component of the solid neoplasm microenvironment. Previous studies demonstrated that hypoxia is involved in glucose metabolism, cell proliferation, apoptosis, autophagy and chemoresistance in various cancers [3]. Hypoxia-inducible factors (HIFs), which are predominant transcription elements responsible for the aforementioned activities, comprise three α-subunits (HIF-1α, HIF-2α and HIF3α) and a β-subunit (HIF-1β). Being one of the most extensively studied HIFs, HIF-1 is a known heterodimer composed of HIF-1β, a cytosolic constitutive subunit, and HIF-1α, a cytoplasmic oxygen-sensitive regulatory subunit [4]. Under normoxic conditions, HIF-1α is mainly localised within the cytoplasm, where it is hydroxylated by oxygen sensors known as prolyl hydroxylase domains (PHDs) and subsequently degraded in a proteasomal manner by Von Hippel-Lindau (VHL)-dependent polyubiquitination. In a hypoxic environment, PHD hydroxylation is suppressed and HIF-1α rapidly accumulates in the cytoplasm before translocating to the nucleus, where it binds to HIF-1β (ARNT) to form a heterodimer, which binds explicitly to hypoxia response elements (HREs) and triggers downstream targeting genes [5]. Accordingly, HIF-1α shares a degree of structural and biochemical similarity with HIF-2α, such as the formation of a heterodimer with HIF-1β (ARNT) [6]. However, numerous studies on HIFs have shown that HIF-2α is only expressed in specific tissues or organs, including endothelium and cardiomyocytes [7]. In contrast, the expression level of HIF-1α is generally detectable in various types of cancer tissues [8]. Aberrant HIF-1α overexpression has been linked to cell survival, epithelial–mesenchymal transition (EMT), and cancer metastasis [9]. For example, it is widely accepted that HIF-1α/VEGF signalling activation promotes tumour vessel formation, which is essential for tumour growth and metastasis [10].

A dysfunctional Wnt pathway, particularly the β-catenin-dependent pathway, is intensively interlinked with the progression

---

[1]Department of Frontier Surgery, Chiba University Graduate School of Medicine, Chiba, Japan. ✉email: t_toyozumi@chiba-u.jp

Received: 5 November 2021 Revised: 3 April 2022 Accepted: 7 April 2022
Published online: 28 April 2022

of diverse cancers [11]. Despite the recent discovery of an interaction between hypoxia and Wnt/β-catenin signalling in neoplasms, this crosstalk is highly inter-tumour heterogeneity. For example, overexpression of HIF-1α under hypoxic stress activates the Wnt/β-catenin pathway and is involved in stemness maintenance in lung adenocarcinoma and glioblastoma [12, 13]. On the contrary, Scholten et al. demonstrated that Wnt/β-catenin signalling is inhibited in human osteosarcoma cells under 0.5% O_2 hypoxic conditions, with HIF-1α playing a central role [14]. Given the limited available information, the role of HIF-1α in ESCC is still unknown and therefore deserves further investigation.

In this research, we assessed the clinical significance of the expression status of HIF-1α, β-catenin, and TCF4/TCF7L2 in ESCC. Furthermore, we characterised the crosstalk between HIF-1α and Wnt/β-catenin signalling in ESCC and elucidated the potential mechanisms.

METHODS

Human ESCC cell lines and chemical reagents

Human ESCC TE cell lines (TE1, TE2, TE5, TE6, TE8, TE9, TE10, TE11 and TE15) were obtained from the Cell Resources Center at Tohoku University. Human ESCC cell line T.Tn was provided by the Japanese Cancer Research Bank. The immortalised oesophageal keratinocyte line R2C3 developed in our laboratory was used as a normal oesophageal cell line [15]. For normoxic conditions, cells were incubated in DMEM/F-12 replenished with 10% FBS and 1% penicillin/streptomycin at 37 °C, 21% O_2 and 5% CO_2. For physical hypoxia, cells were incubated at 1% O_2 and 5% CO_2 in a multi-gas incubator (#BL-43MD, TOSC). For chemical-induced hypoxia, $CoCl_2$ (#C8661, Sigma-Aldrich) was diluted with the experimental medium at a working concentration of 100 μM according to previously reported methods [16, 17]. iCRT14 (#SML0203, Sigma-Aldrich), a β-catenin/TCF inhibitor, was diluted with the experimental medium at the indicated concentrations.

Clinical ESCC tissue samples

We surveyed patients with oesophageal cancer who underwent esophagectomy at Chiba University Hospital between 2004 and 2013. Survival information of patients was summarised in July 2018. The criteria for inclusion of patients in this study were as follows, (a) postoperative pathological diagnosis of ESCC, (b) absence of any other type of cancer (including mixed tumours such as basaloid squamous cell carcinoma and oesophageal adenocarcinoma), (c) not receiving any chemoradiotherapy treatment preoperatively and (d) achieving pathological R0 curative resection. After excluding patients who did not meet the above criteria, we obtained 69 ESCC patients and collected corresponding postoperative frozen tumours and adjacent non-tumour tissues, and paraffin-embedded tumour sections. This research was authorised by the Institutional Review Board of Chiba University (No. 1120-942), and all participants provided written informed consent.

Western blot analysis

Western blot analyses were carried out as previously depicted [18]. Specifically, for physical hypoxia (1% O_2) treated cell samples, cell lysis occurred quickly (within 2 min) once removed from hypoxia (1% O_2). The primary antibodies, anti-human HIF-1α (1:1000, ab1), β-catenin (1:5000, ab32572), β-actin (1:1000, ab115777) were obtained from Abcam (Cambridge, USA). Anti-human E-cadherin (1:1000, sc8426), Snail (1:1000, sc271977), and TCF4/TCF7L2 (1:500, sc166699) primary antibodies were obtained from Santa Cruz Biotechnology (CA, USA). Anti-human N-cadherin (1:1000, CST13116) was purchased from Cell Signaling Technology (MA, USA). β-actin was used as a loading control. Protein signals were examined using an ECL chemiluminescence kit from GE Healthcare (Buckinghamshire, UK).

Quantitative real-time polymerase chain reaction (qRT-PCR)

Total RNA was extracted from ESCC tissues and cell lines using Trizol reagent (Invitrogen) and reversed to cDNA based on a High-Capacity RNA-to-DNA^{TM} Kit (Thermo Fisher Scientific). The qRT-PCR assay was carried out according to a previously reported protocol [18]. The primers used in this analysis are listed in Supplementary Table S1. The fold changes in the expression of each target gene were determined by the comparative threshold cycle (Ct) method with the formula $2^{-\Delta\Delta Ct}$ method [19].

Transfection of the small hairpin (sh)RNA lentiviral particles

HIF-1α shRNA (h) lentiviral particles (sc-35561-V, Santa Cruz) are transduction via viral particles containing 3–5 HIF-1α-specific constructed shRNA designed to knock down HIF-1α gene expression in human cells. HIF-1α shRNA (h) lentiviral particles were transfected into ESCC cell lines to silence HIF-1α according to the manufacturer's protocol. Generally, 5×10^4 ESCC cells were inoculated into six-well plates for 24 h prior to lentiviral infection. Then cells were transfection by 20 μL (Multiplicity of infection, MOI = 2) HIF-1α shRNA (h) lentiviral particles in the presence of 5 μg/ml hexadimethrine bromide (polybrene) (sc-134220, Santa Cruz), and cells were incubated in the transfection system for 12 h. For 10 days, 10 μg/ml puromycin dihydrochloride (sc-108071, Santa Cruz) was used continuously to obtain stable HIF-1α knockdown T.Tn and TE1 cell lines. Control shRNA lentiviral particles (sc-108080, Santa Cruz) were used as a negative control to exclude the effect of viral particle vectors. CopGFP control lentiviral particles (sc108084, Santa Cruz) were employed to evaluate transduction efficiency and determine the optimal MOI.

Cell proliferation and cytotoxicity assays

Cell counting kit-8 (Dojindo Molecular Technologies, Japan) was used to evaluate proliferation from 6–120 h after ESCC cells were seeded into a 96-well plate (1×10^3 cells/100 μL media). For cell viability assay, ESCC cells were inoculated into 96-well plates with conditioned medium containing graded dilutions of 5-fluorouracil (0–10,000 μM) or Cisplatin (0–100 μM) under normoxic or hypoxic (1% O_2 or 100 μM $CoCl_2$) conditions for 48 h.

Transwell assays

Migration/invasion capacity was detected via transwell experiments as previously described [18]. Generally, two models of schedules are employed, after 24 h (migration) or 30 h (invasion) of incubation in $CoCl_2$ treatment groups, cells attached to the lower side were stained and fixed with a Diff-Quick Stain kit (International Reagents, Japan). Photos of three random fields from three replicated wells were obtained and cells were counted. Besides, for the hypoxia (1% O_2) treatment groups, 24-well transwell chambers (8-μm pore size, #662638, Greiner Bio-One) with or without Matrigel (#354236, Corning) were applied to assess the migration and invasion abilities. The incubation time for migration and invasion was adjusted to 30 and 48 h, respectively.

Cell apoptosis/cycle analysis

The cell apoptosis analyses were performed according to the scheme of Annexin V-FITC Apoptosis Detection Kit (#V9G5609, Nacalai Tesque, Japan). The total apoptotic rate was calculated by adding the early and late apoptotic rates. For cell cycle analyses, cells were pre-conditioned in non-serum media for 24 h. In all, 5×10^5 cells/tube were fixed in 70% ethanol for 24 h at 4 °C before being reacted with 50 μg/ml propidium iodide (100 μg/ml RNaseA, 0.1% Triton X-100) for 30 min at room temperature in darkness. All specimens were processed using BD FACS Canto II (BD Biosciences).

Cell immunofluorescence (IF) staining assay

Cells were fixed in ice-cold 4% polyphosphate formaldehyde and then permeabilized in 0.1% Triton X-100. The fixed cells were blocked with 5% bovine serum albumin and incubated with the following primary antibodies: anti-E-cadherin (1:100, sc8426), anti-N-cadherin (1:100, CST13116) and anti-Snail (1:100, sc271977). Before fluorescence imaging with a fluorescence microscope, 4′,6-diamidino-2-phenylindole was added.

Co-immunoprecipitation (co-IP) assay

The co-IP assay was conducted using the Dynabeads Protein G Immunoprecipitation Kit (#1639291, Novex). Generally, anti-β-catenin (ab32572, Abcam) or anti-HIF-1α (ab1, Abcam) antibodies were conjugated with magnetic beads to generate the magnetic bead-Ab compounds, followed by incubation with cell lysate in each group (containing an equal amount of proteins) to enable conjugation of the target protein to the magnetic bead-Ab compounds. Elution buffer was used to elute target proteins. Harvested samples were further analysed by western blotting analysis.

Chromatin immunoprecipitation qRT-PCR assay (ChIP-qRT-PCR)

The Simple ChIP Plus Enzymatic Chromatin IP Kit (#9055, Cell Signaling Technology) was used to carry out the ChIP assays according to the manufacturer's guidelines. Enrichment of promoter was quantified using qRT-PCR on the percentage of ChIP-eluted DNA versus input. Isotype IgG was served as an immunoprecipitation negative control. For the qRT-PCR assay, the HIF-1α binding site, alternatively termed as hypoxia-responsive element (HRE) motifs (5′-(A/G)CGTG-3′) on human TCF4/TCF7L2 promoter region (GenBank: AF522996.1) were estimated via the JASPAR database (http://jaspar.genereg.net). We characterised the putative hypoxia response element (HRE) within the human TCF4/TCF7L2 proximal promoter region (NC_000010.11:c112950191-112950182). The specific walking primers for the ChIP-qRT-PCR assay were designed as follows: TCF4/TCF7L2 forward, 5′-CTCGTGCCGCTCGGATTT-3′; reverse, 5′-CGCCGCCTTTGAACTGA-A-3′.

Tumour xenograft model

Our animal research was approved by the Animal Care and Use Committee of Chiba University (No. A3-22).

A total of 20 6–8-week-old female thymus-free nude mice (nu/nu) were purchased from the Animal Maintenance Facility of Chiba University and housed under specific pathogen-free conditions. Twenty mice were randomly divided into four groups (*n* = 5 per group). In all, 5×10^6 Nc-sh or HIF-1α-sh T.Tn cells were mixed with 100 µL PBS and inoculated subcutaneously into the right anterolateral thigh of nude mice. Tumour volume ($V = \text{width}^2 \times \text{length}/2$, mm^3) and body weight (g) of nude mice were recorded every three days. One week later, subcutaneous graft tumours were palpable, and the corresponding subgroup of nude mice received intraperitoneal injections of 5-fluorouracil (5-FU) (20 mg/kg, every 3 days), control nude mice were injected intraperitoneally with 1% DMSO every 3 days for 21 days. Measurements and injections were carried out sequentially according to cage numbers and remained consistent throughout the study. All mice were sacrificed by cervical dislocation under phenobarbital anaesthesia. The isolated tumours were weighed, photographed, and fixed in 10% formalin for subsequent experiments.

The tumour growth inhibition rate (TGI%) was calculated as previously described [20]. The specific formula is as follows, $[1\text{-}(V_{T21}–V_{T0}) = \text{mean } (V_{C21}–V_{C0})] \times 100$, with V_{T21} and V_{T0} referring to the tumour volumes of animals in the drug-treated group at days 21 and 0, and V_{C21} and V_{C0} referring to the tumour volumes of animals in the control group at days 21 and 0.

Immunohistochemistry (IHC) and assessment

Immunohistochemistry was performed on paraformaldehyde-fixed paraffin-embedded ESCC sections. The HIF-1α (1:150, ab1), β-catenin (1:250, ab32572), and TCF4/TCF7L2 (1:20, sc166699), Ki67 (1:100, #M7240, Dako), CD31 (1:100, ab124432) primary antibodies were used for immunohistochemistry by streptavidin peroxidase method. The procedure was performed as previously reported [18]. Protein expression levels were evaluated independently by two investigators in the presence of a pathologist, all of them were blinded to the patient clinical information. The method of evaluating IHC staining results was as follows: intensity score: 0, none; 1, weak; 2, moderate; 3, strong; percentage score: 0% ≤0 < 5%; 5% ≤1 < 25; 25% ≤2 < 50%; 50% ≤3 < 75%; 75% ≤4 < 100%. The final IHC score is equal to the intensity score multiplied by the percentage score. The positive IHC results for HIF-1α, β-catenin and TCF4/TCF7L2 were determined to be the final IHC score of 1 + , 3 + and 2+ respectively. CD31 was adopted as a vascular endothelial cells marker. The counts of CD31-positive labelled microvessels were determined based on previous reports [21].

Statistical analysis

The data in this study are expressed as means ± standard deviations (SDs). The F-test was performed to evaluate sample variance. The Student's *t* test or Welch's *t* test was used to compute statistical significance between the two experimental groups. One-way analysis of variance (ANOVA) followed by Dunnet's post test was used to analyse three or more groups. Spearman's rank correlation coefficient was used to assess linear correlations. Kaplan–Meier survival curves were examined using Log-rank (Mantel–Cox) test. Statistical analysis was carried out using GraphPad Prism software (version 9.0.0). *P* values <0.05 were considered statistically significant.

RESULTS

Hypoxia and HIF-1α shRNA regulates HIF-1α expression in ESCC cell lines

We initially quantified HIF-1α mRNA and protein levels in ten ESCC cell lines compared to an oesophageal epithelium R2C3 under normoxic conditions before identifying the biological features of HIF-1α. T.Tn and TE1 cell lines had a relatively significant abundance of mRNA and protein levels of HIF-1α, hence they were selected for subsequent experiments (Fig. 1a). Next, we observed that 1% O_2 treatment upregulated HIF-1α mRNA expression in a time-dependent manner, with the peak occurring at 24 h (T.Tn) and 12 h (TE1), the HIF-1a mRNA expression of T.Tn and TE1 cells which simultaneously exposed to 1% O_2 decreased at 48 and 24 h, respectively (Fig. 1b). Furthermore, we discovered that $CoCl_2$ (100 µM, 24 h) considerably upregulates HIF-1α mRNA in T.Tn and TE1 cells when compared to the normoxic baseline (Fig. 1c, d). As shown in Fig. 1e, f, HIF-1α protein was also upregulated in T.Tn and TE1 cells in the presence of 1% O_2 or $CoCl_2$. Interestingly, we also found that either 1% O_2 or $CoCl_2$ treatment upregulated HIF-1α mRNA expression in R2C3 cells (Supplementary Fig. 1A).

Next, significant differences between normoxic control and HIF-1α-shRNA knockdown T.Tn and TE1 cells were revealed when the efficiency of HIF-1α-shRNA in T.Tn and TE1 cells was confirmed using qRT-PCR (Fig. 1c, d) and western blot (Fig. 1e, f). In addition, compared to the hypoxic baseline, 1% O_2 or $CoCl_2$ induced upregulation of HIF-1α mRNA and protein expression in T.Tn and TE1 cells was noticeably abrogated in the presence of HIF-1α-shRNA treatment (Fig. 1c–f).

HIF-1α promotes ESCC cell proliferation, migration and invasion in vitro

We evaluated the proliferation ability of ESCC cells in the presence of either normoxia or physical hypoxia (1% O_2) or chemical hypoxia ($CoCl_2$) between 6 and 120 h to examine whether hypoxia influences ESCC cell proliferation. We found that physical hypoxia (1% O_2) inhibited the proliferation of T.Tn and TE1 cells when compared to normoxic conditions (Fig. 2a, b). Interestingly, contrary to this observation, $CoCl_2$ treatment promoted proliferation in both T.Tn and TE1 cells (Fig. 2c, d). We then characterised the effect of HIF-1α knockdown on ESCC cell proliferation. Knockdown of HIF-1α had a significant inhibitory impact on T.Tn and TE1 cell proliferation in either normoxia, physical hypoxia (1% O_2), or chemical hypoxia ($CoCl_2$) (Fig. 2a–d). In addition, we also investigated the effect of hypoxia (1% O_2 and $CoCl_2$) on the proliferative capacity of R2C3 cells, as shown in Supplementary Fig. 1B, the proliferation capacity of R2C3 cells was significantly decreased in the presence of 1% O_2 exposure, while, R2C3 cell proliferation capacity did not show significant changes under $CoCl_2$ treatment.

Figure 2e, f shows that both 1% O_2 exposure and $CoCl_2$ treatment enhanced the migratory and invasion capacities of T.Tn and TE1 cells, whereas HIF-1α inhibition had the opposite effect when compared to normoxic control. Meanwhile, quantification of either 1% O_2 exposure or $CoCl_2$-induced migration and invasion was visibly reversed in the presence of HIF-1α shRNA in comparison to the hypoxic control group (Fig. 2e, f). Meanwhile, we did not observe significant changes in the migratory and invasive ability of R2C3 cells in 1% O_2 and $CoCl_2$ mimic hypoxic environment (Supplementary Fig. 1C).

$CoCl_2$ inhibits apoptosis and accelerates cell cycle progression in a HIF-1α-dependent manner

Because apoptosis and cell cycle arrest often contribute to decreased cell proliferation, we investigated whether HIF-1α can modulate ESCC cell lines apoptosis and cell cycle progression. We used FACS analysis to detect the apoptosis (Fig. 2g, h) and cell cycle distribution (Fig. 2i, j) of T.Tn and TE1 cells. The results indicated that $CoCl_2$ suppressed cell apoptosis and accelerated cell cycle progression in T.Tn and TE1 cells by decreasing the distribution of G0/G1 interphase cells. On the contrary, HIF-1α knockdown upregulated the proportion of apoptotic cells and the ratio of cells in G0/G1 interphase compared to normoxic baseline. Furthermore, $CoCl_2$-induced apoptosis inhibition and cell cycle

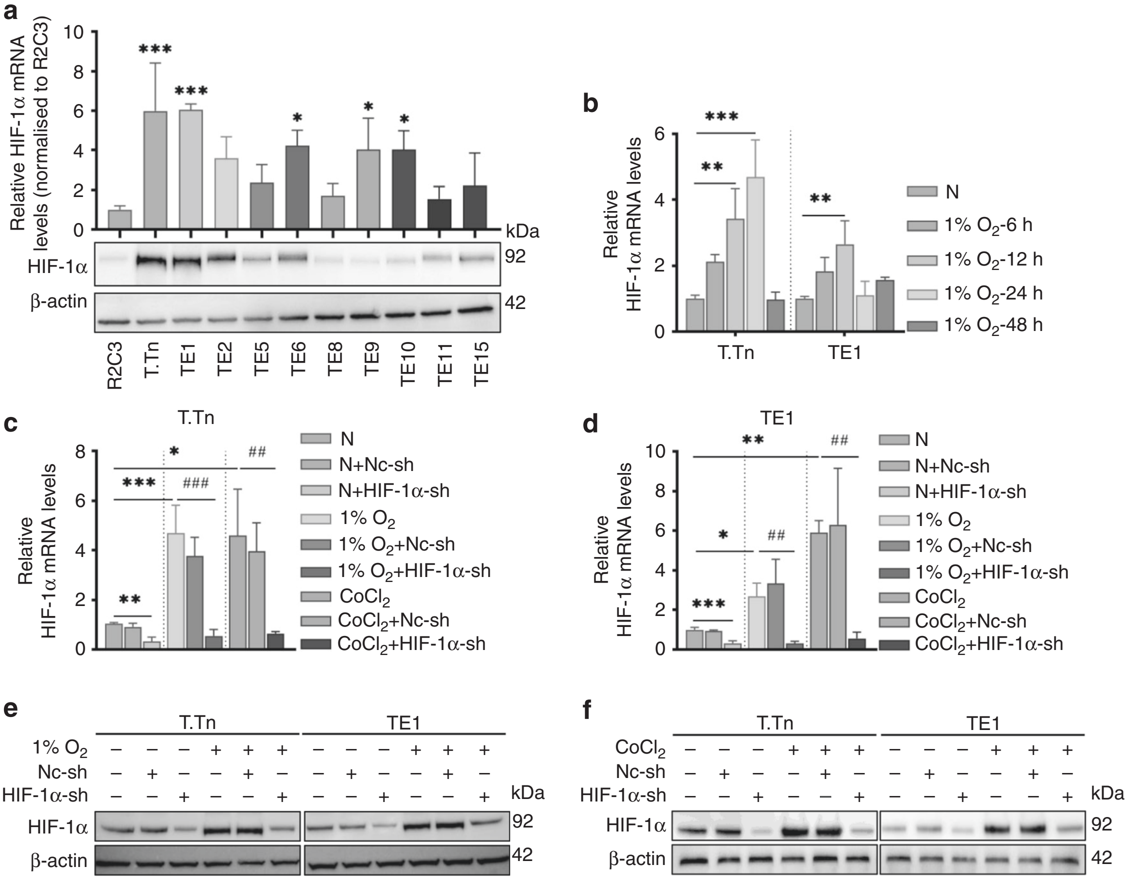

Fig. 1 1% O_2 or $CoCl_2$ induced hypoxia and HIF-1α shRNA regulating HIF-1α expression in ESCC cell lines. **a** mRNA and protein levels of HIF-1α in ESCC cell lines and an oesophageal keratinocyte R2C3. **b** HIF-1α mRNA levels at different time points in T.Tn and TE1 cells in 1% O_2 condition. **c**, **d** HIF-1α mRNA levels in 1% O_2 (T.Tn, 24 h; TE1, 12 h) or $CoCl_2$ (100 μM, 24 h) induced hypoxia and HIF-1α shRNA-mediated knockdown of HIF-1α in T.Tn and TE1 cell lines, respectively. Data were normalised to normoxia. **e**, **f** HIF-1α protein content of in the above indicated groups. All data represent mean ± SD of three independent experiments. $^{*}P < 0.05$, $^{**}P < 0.01$, $^{***}P < 0.001$ vs normoxic baseline. $^{\#}P < 0.05$, $^{\#\#}P < 0.01$, $^{\#\#\#}P < 0.001$ vs hypoxic (1% O_2 or $CoCl_2$) baseline. N normoxia, Nc-sh negative control shRNA, HIF-1α-sh HIF-1α-shRNA.

motivation in T.Tn and TE1 cells were partially reversed in the presence of HIF-1α shRNA when compared to the hypoxic baseline. Together, these findings indicated the critical role of HIF-1α in regulating the viability of ESCC cells in vitro.

Hypoxia-induced EMT in oesophageal squamous cancer is specifically associated with HIF-1α

Epithelial–mesenchymal transition (EMT) activation is involved in promoting the ability of tumour cells to invade, metastasis, and acquire tumour-initiating cells (TICs) potential [22]. The goal of this study was to investigate the role of HIF-1α in the EMT state of ESCC cells. Firstly, we examined the mRNA and protein expression of two representative EMT markers and one EMT transcription factor (EMT-TF). According to Fig. 3a, b, 1% O_2 and $CoCl_2$-simulated hypoxia significantly decreased the mRNA content of the epithelial marker E-cadherin while increasing the mRNA content of the mesenchymal marker N-Cadherin. Meanwhile, the EMT-TF, Snail, was upregulated under 1% O_2, and $CoCl_2$ mimic the hypoxia environment. In contrast, HIF-1α knockdown led to an increase in E-cadherin and a decrease in N-cadherin under normoxic condition. Consistently, HIF-1α knockdown notably lowered the mRNA expression level of EMT-TF, Snail, compared to the normoxic baseline. Furthermore, 1% O_2 and $CoCl_2$ mimic hypoxia-induced EMT activation was partially abolished in the presence of HIF-1α specific shRNA when compared to the hypoxic baseline (Fig. 3a, b). Moreover, the impact of HIF-1α on the EMT progression of T.Tn and TE1 cells were validated by the results of western blot assay (Fig. 3c, d) and immunofluorescence staining (Fig. 3e, f). Besides, the mRNA levels of E-cadherin, N-cadherin and Snail in R2C3 cells did not show significant changes in the 1% O_2 and $CoCl_2$ induced hypoxic environment (Supplementary Fig. 1D). Collectively, our findings suggest that HIF-1α functions in accelerating the progression of EMT in ESCC in vitro.

HIF-1α mediates the resistance of ESCC cell lines to 5-fluorouracil (5-FU) in vitro and in vivo

The role of HIF-1α in hypoxia-induced Cisplatin or 5-fluorouracil (5-FU) chemoresistance in ESCC has not been previously reported. To investigate the mechanism by which hypoxia affects the drug sensitivity of ESCC cells, we examined the viability of T.Tn and TE1 cells after 48 h of incubation with different concentrations of Cisplatin and 5-fluorouracil (5-FU) under normoxic, 1% O_2 and $CoCl_2$ mimic hypoxic conditions. As shown in Supplementary Fig. 2A, B, 1% O_2 exposure significantly decreased the cytotoxicity of 5-fluorouracil (5-FU) on T.Tn and TE1 cells compared to those cultured in normoxic conditions. However, 1% O_2 exposure was not sufficient to induce Cisplatin resistance in T.Tn and TE1 cells (Supplementary Fig. 2D, E). Meanwhile, $CoCl_2$ treatment also resulted in 5-fluorouracil (5-FU) resistance enhanced in T.Tn and TE1 cells (Supplementary Fig. 2G, H). Similarly, there was no significant effect on the response of Cisplatin in the presence of $CoCl_2$ (Supplementary Fig. 2J, K). The corresponding IC_{50} values of 5-fluorouracil (5-FU) or Cisplatin for T.Tn and TE1 cells were shown in Supplementary Fig. 2C, F, I, L. To investigate if HIF-1α is responsible

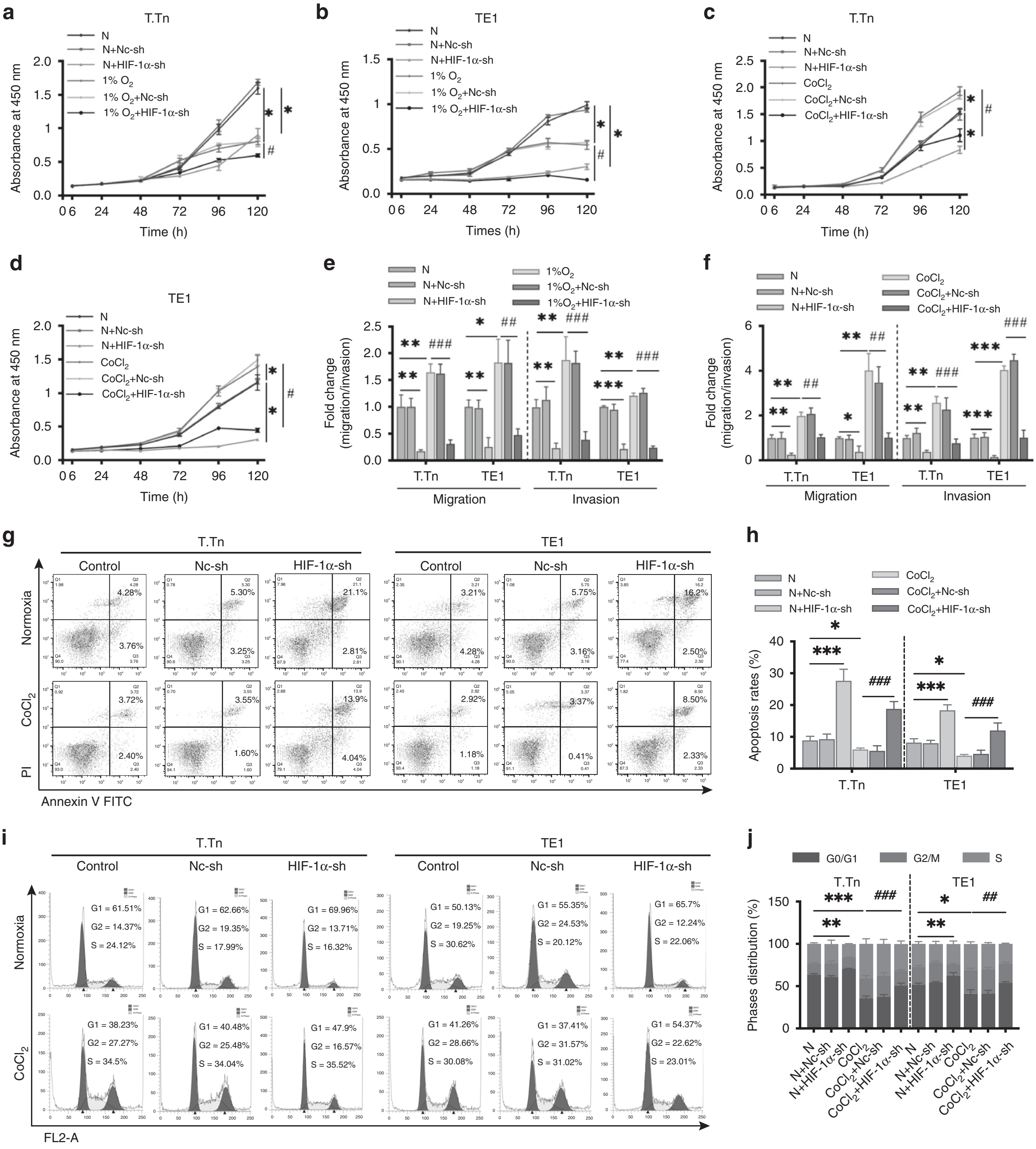

Fig. 2 The role of HIF-1α in ESCC cell proliferation, migration, invasion, apoptosis and cell cycle in vitro. **a**, **b** The proliferation of T.Tn and TE1 cells with or without HIF-1α knockdown cultured in normoxic and hypoxic (1% O_2) conditions for 6–120 h. **c**, **d** The proliferation of T.Tn and TE1 cells with or without HIF-1α knockdown cultured in a normoxic environment and $CoCl_2$ treatment 6–120 h. **e**, **f** The impact of HIF-1α on the migratory and invasive capacity of the indicated cells. Data was normalised to normoxia. **g**, **h** Apoptosis rates and representative pictures in T.Tn and TE1 cells expressing a negative control-shRNA or HIF-1α shRNA in normoxia for 24 h with or without $CoCl_2$ (100 μM). **i**, **j** The cell cycle distribution in the indicated T.Tn and TE1 cells in normoxia for 24 h with or without $CoCl_2$ (100 μM). The bar graph shows the statistically significant difference in the G0/G1 phase. All data represent mean ± SD of three independent experiments. $^{*}P < 0.05$, $^{**}P < 0.01$, $^{***}P < 0.001$ vs normoxic baseline. $^{\#}P < 0.05$, $^{\#\#}P < 0.01$, $^{\#\#\#}P < 0.001$ vs hypoxic (1% O_2 or $CoCl_2$) baseline. N normoxia, Nc-sh negative control shRNA, HIF-1α-sh HIF-1α-shRNA.

for hypoxia-induced 5-fluorouracil (5-FU) resistance, shRNA-mediated knockdown of HIF-1α was followed by 5-fluorouracil (5-FU) treatment. As shown in Fig. 4a, b and Supplementary Fig. 2G, H, after knocking down HIF-1α, the survival rate of 5-fluorouracil (5-FU) treated ESCC cells was drastically reduced in both normoxic and hypoxic (1% O_2 and $CoCl_2$) environments. The corresponding IC_{50} analysis is shown in Fig. 4c and Supplementary Fig. 2I. In addition, we also examined whether hypoxic (1% O_2 and $CoCl_2$)

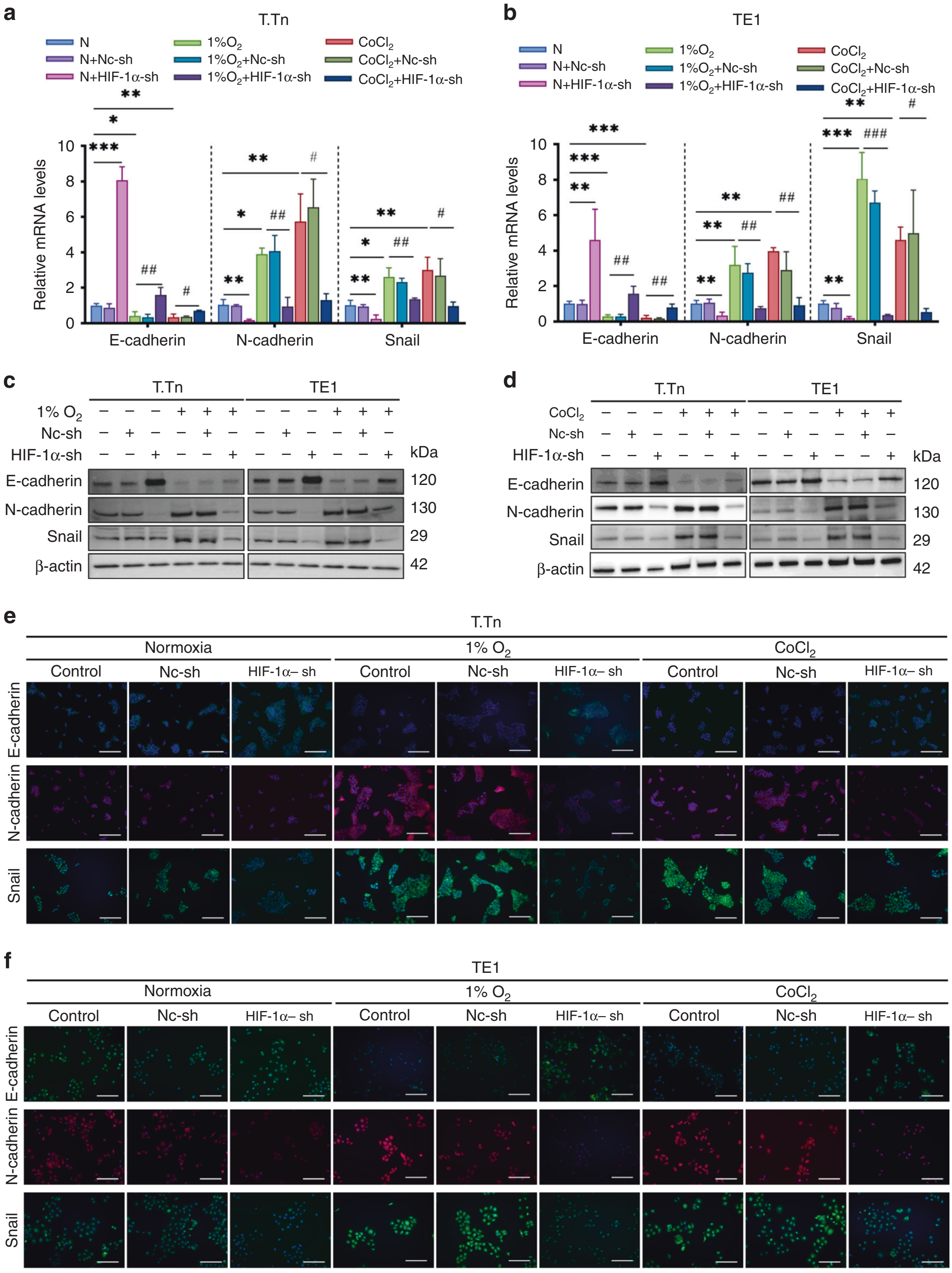

Scar bar: 100 μm

Fig. 3 HIF-1α was involved in hypoxia-induced EMT activation in T.Tn and TE1 cell lines. T.Tn and TE1 cells with or without HIF-1α knockdown were cultured under normoxia, 1% O_2 (T.Tn, 24 h; TE1, 12 h) exposure, and $CoCl_2$ (100 μM, 24 h) treatment. The mRNA (**a**, **b**) and protein (**c**, **d**) levels of E-cadherin, N-cadherin and Snail of the indicated T.Tn and TE1 cells. **e**, **f** The expression of E-cadherin, N-cadherin and Snail in the indicated T.Tn and TE1 cells, were detected using immunofluorescence. E-cadherin and Snail were stained green, N-cadherin was stained red, and the nuclei were stained blue with DAPI. Data were normalised to normoxia. All data represent mean ± SD of three independent experiments. $^{*}P < 0.05$, $^{**}P < 0.01$, $^{***}P < 0.001$ vs normoxic baseline. $^{\#}P < 0.05$, $^{\#\#}P < 0.01$, $^{\#\#\#}P < 0.001$ vs hypoxic (1% O_2, $CoCl_2$) baseline. Scar bar: 100 μm. N normoxia, Nc-sh negative control shRNA, HIF-1α-sh HIF-1α-shRNA.

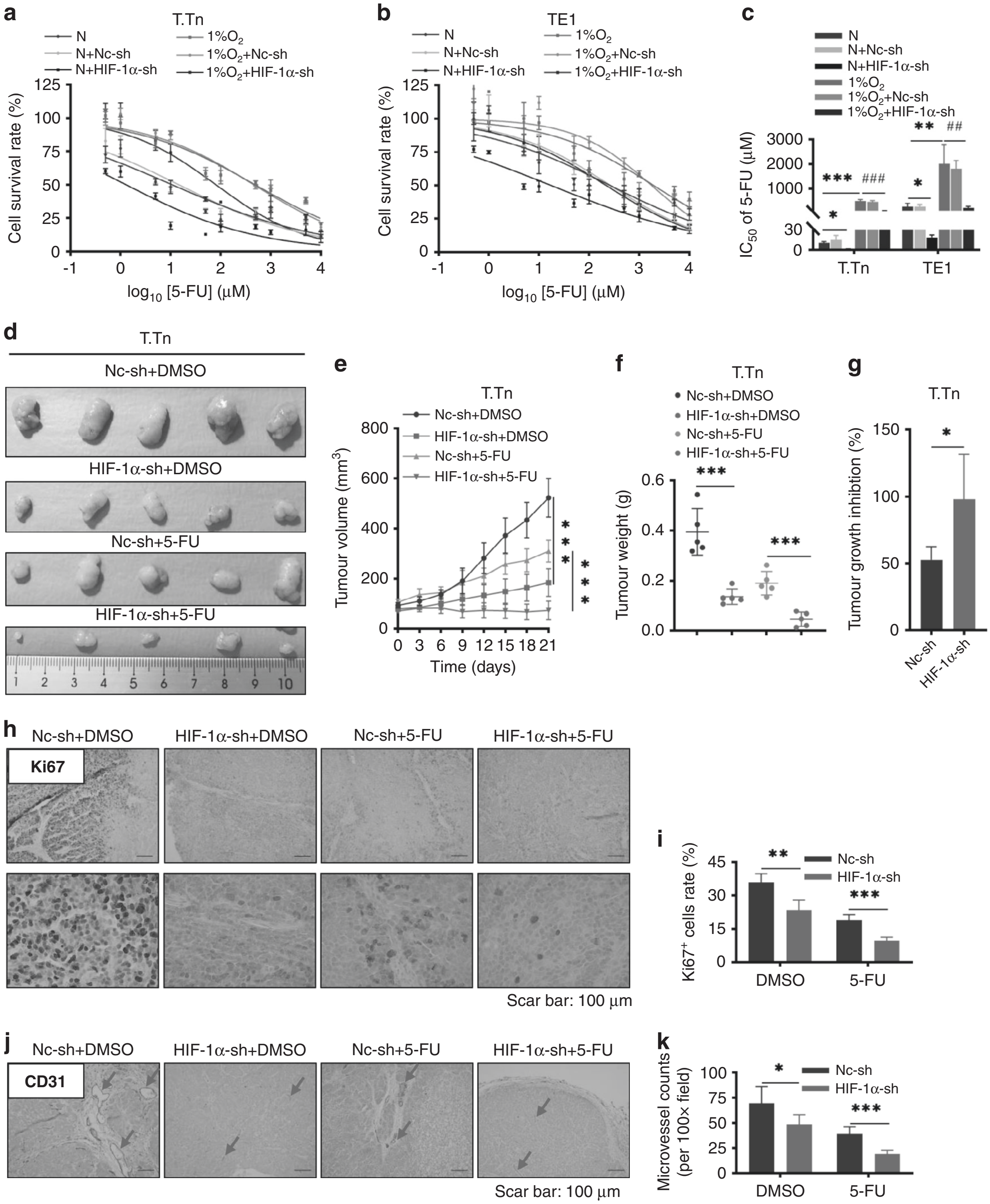

Fig. 4 HIF-1α mediated the resistance of ESCC cell lines to 5-FU in vitro and in vivo. **a**, **b** Effect of different concentrations of 5-fluorouracil (5-FU) (0–10,000 μM) on cell viability in indicated T.Tn and TE1 cells with or without HIF-1α knockdown under normoxic and hypoxic (1% O_2) conditions for 48 h. **c** The corresponding IC_{50}. All data represent mean ± SD of three independent experiments. $^*P < 0.05$, $^{**}P < 0.01$, $^{***}P < 0.001$ vs normoxic baseline. $^{\#}P < 0.05$, $^{\#\#}P < 0.01$, $^{\#\#\#}P < 0.001$ vs hypoxic (1% O_2) baseline. **d** Representative photographs of T.Tn xenograft tumours in nude mouse with different treatments in four groups (Nc-sh + DMSO, HIF-1α-sh + DMSO, Nc-sh + 5-FU, HIF-1α-sh + 5-FU, *n* = 5 per group) after 21 days. **e** T.Tn xenograft tumour regression curves based on tumour volume (mm^3) in four groups of nude mice with 1% DMSO or 5-fluorouracil (5-FU) (20 mg/kg) treatments after 21 days. **f** T.Tn xenograft tumour weight (g) following different treatments in four groups after 21 days. **g** Tumour growth inhibition (TGI) at the 21th days following 5-fluorouracil (5-FU) treatment in T.Tn xenograft tumour models with or without HIF-1α knockdown. **h**, **i** Positive ratio of Ki67 expression cells in T.Tn xenograft tumours in four different treatment groups, representative pictures achieved by immunohistochemistry (×40 (upside) and ×100 (downside)), and corresponding bar charts. **j**, **k** Angiogenesis analysis in T.Tn xenograft tumours in four different treatment groups, representative pictures achieved by immunohistochemistry (×40), and corresponding microvessel counts bar charts. Scar bar: 100 μm. $^*P < 0.05$, $^{**}P < 0.01$, $^{***}P < 0.001$, unpaired *t* test, two-tailed test. N normoxia, Nc-sh negative control shRNA, HIF-1α-sh HIF-1α-shRNA, 5-FU 5-fluorouracil, DMSO dimethylsulfoxide.

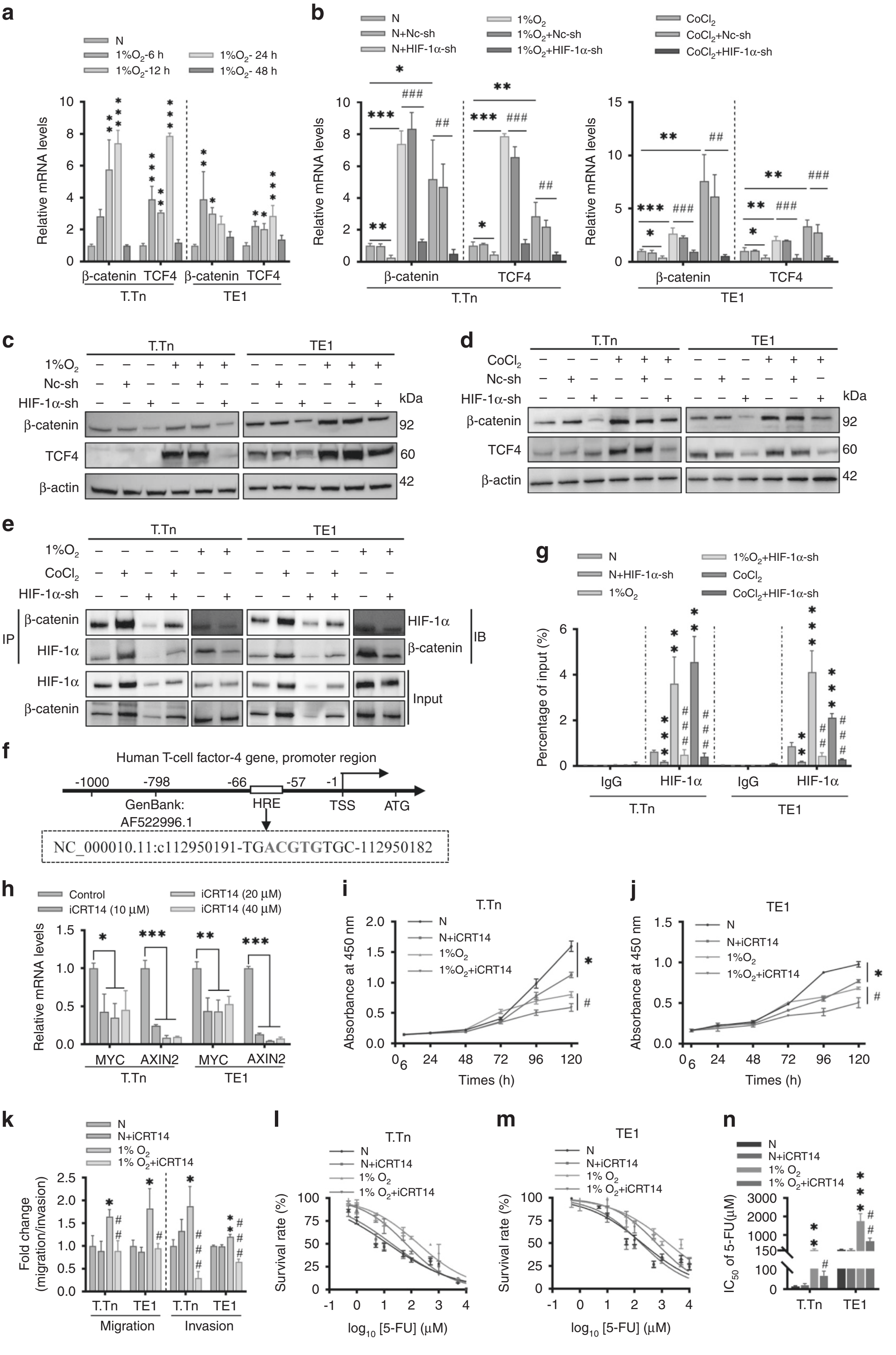

environments modulate the response of R2C3 cells to Cisplatin and 5-fluorouracil (5-FU), the viability of Cisplatin or 5-fluorouracil (5-FU)-treated R2C3 cells did not show significant changes in the hypoxic environment, compared with the normoxic environment (Supplementary Fig. 1E–H).

To explore the role of HIF-1α in 5-fluorouracil (5-FU) resistance in vivo, T.Tn subcutaneous xenograft nude mouse model was established (Supplementary Fig. 3A), HIF-1α expression in xenograft tumours was altered by subcutaneous injection of HIF-1α-shRNA expressing T.Tn cells (Supplementary Fig. 3C, D). Our

Fig. 5 Crosstalk between HIF-1α and Wnt/β-catenin signalling pathway in ESCC cell lines. **a** β-catenin and TCF4/TCF7L2 mRNA levels in T.Tn and TE1 cells at different time points under 1% O_2 exposure. **b** The mRNA levels of β-catenin and TCF4/TCF7L2 were detected T.Tn and TE1 cell lines with or without HIF-1α shRNA transfection in the presence of 1% O_2 (T.Tn, 24 h; TE1, 12 h) or $CoCl_2$ (100 μM, 24 h). Data were normalised to normoxia. **c**, **d** Western blot assays for β-catenin and TCF4/TCF7L2 protein expression were performed in the indicated cells as described above. **e** The physical association between HIF-1α and β -catenin in indicated T.Tn and TE1 cells is based on co-immunoprecipitation (Co-IP) blotting. **f** Schematic representation of the human TCF4/TCF7L2 promoter region. **g** The relative abundance of HIF-1α binding to the TCF4/TCF7L2 promoter in indicated T.Tn and TE1 cells was measured by ChIP. ChIP-qRT-PCR quantitation was shown as % relative to input, IgG was used as a negative control. **h** The relative mRNA levels of MYC and AXIN2 in iCRT14-treated T.Tn and TE1 cells at the indicated concentrations under normoxic conditions. Effects of iCRT14 (10 μM, 24 h pretreatment) on cell proliferation (**i**, **j**), migration/invasion (**k**), 5-fluorouracil (5-FU) resistance (**l**, **m**) in T.Tn and TE1 cells cultured in normoxic and hypoxic (1% O_2) environments. **n** Corresponding IC_{50}. All data represent mean ± SD of three independent experiments. $^*P < 0.05$, $^{**}P < 0.01$, $^{***}P < 0.001$ vs normoxic baseline. $^{\#}P < 0.05$, $^{\#\#}P < 0.01$, $^{\#\#\#}P < 0.001$ vs hypoxic (1% O_2 or $CoCl_2$) baseline. TSS transcription starting site, HRE hypoxia-responsive element, N normoxia, Nc-sh negative control shRNA, HIF-1α-sh HIF-1α-shRNA.

results indicated no significant difference in body weight among the four different treatment groups of nude mice (Supplementary Fig. 3B), but intraperitoneal injection of 5-fluorouracil (5-FU) significantly decreased subcutaneous tumour volume and weight compared to the DMSO intraperitoneal control group, and knockdown of HIF-1α further reduced subcutaneous tumour volume and weight (Fig. 4d–f). As expected, T.Tn xenograft tumours were resistant to 5-fluorouracil (5-FU) (%TGI: 52.6% ± 9.8%), while the combination of HIF-1α-shRNA with 5-fluorouracil (5-FU) synergistically strengthened tumour growth inhibition (% TGI: 98.0% ± 33.6%) (Fig. 4g).

Immunohistochemical staining further showed that protein level of proliferation marker Ki67 (Fig. 4h, i) and microvessel counts (endothelial cell marker CD31-positive label, Fig. 4j, k) in T.Tn xenograft tumours were reduced in the intraperitoneal 5-fluorouracil (5-FU) treatment group compared with the DMSO control group, while the inhibitory effect of 5-fluorouracil (5-FU) was further amplified in the combination treatment (5-fluorouracil (5-FU) + HIF-1α-shRNA). Besides, the protein level of β-catenin and TCF4/TCF7L2 in T.Tn xenograft tumours were reduced in the HIF-1α-shRNA group compared with the Nc-shRNA control group, and the combination of HIF-1α-shRNA with 5-fluorouracil (5-FU) further decreased the protein level of TCF4/TCF7L2 but not β-catenin, suggesting that TCF4/TCF7L2 may be involved in HIF-1α-mediated 5-fluorouracil (5-FU) resistance (Supplementary Fig. 3E–H).

Activation of Wnt/β-catenin signalling under hypoxia promotes ESCC progression

Previous studies have demonstrated that HIF-1α was a predominant component of hypoxic adaptation that regulated the Wnt/β-catenin signalling in mouse hypoxic embryonic stem cells by augmenting β-catenin activation and expression of the downstream effector lymphoid enhancer-binding factor-1/T-cell factor-1 (LEF-1/TCF-1) [23]. Recent research has also shown that the Wnt/β-catenin signalling pathway is associated with various aspects of hypoxia-mediated human tumour progression, including invasiveness, EMT and metastasis [24–26].

Therefore, we sought to clarify whether β-catenin and TCF4/TCF7L2, which are pivotal intranuclear effectors of the carcinogenic Wnt/β-catenin signalling pathway, could be augmented in ESCC cell lines by hypoxia. As predicted, our data showed that mRNA levels of β-catenin and TCF4/TCF7L2 in T.Tn cells increased significantly in response to hypoxia (1% O_2) in a time-dependent manner, with the peak occurring at 24 h (consistent with HIF-1α), compared with normoxia (Fig. 5a). However, the time points at which mRNA levels of β-catenin and TCF4/TCF7L2 peaked under hypoxia (1% O_2) in TE1 cells were inconsistent (6 and 24 h, respectively) (Fig. 5a), so we selected the time point of HIF-1α mRNA peak expression (12 h) to continue the mechanistic study (Fig. 1b). Furthermore, significant induction of β-catenin and TCF4/TCF7L2 after $CoCl_2$ treatment was observed (Fig. 5b). In addition, the mRNA or protein content of β-catenin and TCF4/TCF7L2 was dramatically reduced in HIF-1α knockdown T.Tn and TE1 cells maintained in normoxia, 1% O_2 exposure or $CoCl_2$ treatment (Fig. 5b–d). In addition, we also investigated the expression of mRNA levels of key regulators of the Wnt/β-catenin signalling pathway, β-catenin and TCF4/TCF7L2 in R2C3 cells under hypoxic (1%O_2, $CoCl_2$) environment and the results showed that hypoxia could not significantly regulate the expression of β-catenin and TCCF4/TCF7L2 in R2C3 cells (Supplementary Fig. 1I).

Using co-immunoprecipitation, the HIF-1α/β-catenin complex was detected in TT.n and TE1 cells, the abundance of the HIF-1α/β-catenin complex was accelerated upon 1% O_2 exposure or $CoCl_2$ treatment and obstructed by HIF-1α shRNA (Fig. 5e). To understand the underlying mechanism of Wnt/β-catenin signalling motivation during hypoxia, the sequence of the promoter region in the TCF4/TCF7L2 gene was further investigated, and identify a putative hypoxia response element (HRE) binding site (at −66 bp/−57 bp) (Fig. 5f). Significant fold enrichment of HIF-1α binding with the HRE of TCF4/TCF7L2 promoter was verified in 1% O_2 exposure or $CoCl_2$ treated T.Tn and TE1 cells using ChIP assay, as well as a considerable decrease in enrichment after HIF-1α knockdown (Fig. 5g).

Next, iCRT14, a β-catenin/TCF complex inhibitor, was used to inhibit the transcriptional activity of β-catenin/TCF. The mRNA content of MYC and AXIN2 was measured in T.Tn and TE1 cells to test the effect of iCRT14 on downstream genes of the Wnt/β-catenin signalling. The 10 μM dosage concentration was chosen because it caused a sufficient reduction in MYC and AXIN2 mRNA expression in both cell lines (Fig. 5h). In functional experiments, 24 h pretreatment with 10 μM iCRT14 inhibited growth in either normoxic or hypoxic (1% O_2, $CoCl_2$) conditions (Fig. 5i, j and Supplementary Fig. 4A, B), and eliminated the facilitation of hypoxic stress on migration and invasion (Fig. 5k and Supplementary Fig. 4C). Furthermore, we investigated the impact of iCRT14 on hypoxia (1% O_2, $CoCl_2$)-induced 5-fluorouracil (5-FU) resistance, and the data showed that iCRT14 pretreatment decreased cell survival when compared to the hypoxic (1% O_2, $CoCl_2$) group (Fig. 5l–n and Supplementary Fig. 4D–F).

Correlation of HIF-1α, β-catenin and TCF4/TCF7L2 expressions in ESCC tissues

To understand the correlation of HIF-1α with the Wnt/β-catenin signalling pathway in ESCC, we quantified the mRNA content of HIF-1α, β-catenin and TCF4/TCF7L2 in 69 pairs ESCC patients with matched neoplastic and adjacent non-neoplastic oesophageal tissue. The mRNA levels of HIF-1α, β-catenin and TCF4/TCF7L2 were significantly elevated in cancerous tissues compared to the corresponding non-tumour oesophageal tissues (Fig. 6a–c), suggesting that both HIF-1α and the Wnt/β-catenin signalling were activated at the transcriptional level during ESCC progression. Furthermore, the level of HIF-1α mRNA was positively correlated with β-catenin or TCF/TCF7L2 in ESCC tissues (Fig. 6d, e). However, there was no significant correlation between β-catenin and TCF/TCF7L2 in ESCC tissues (Fig. 6f).

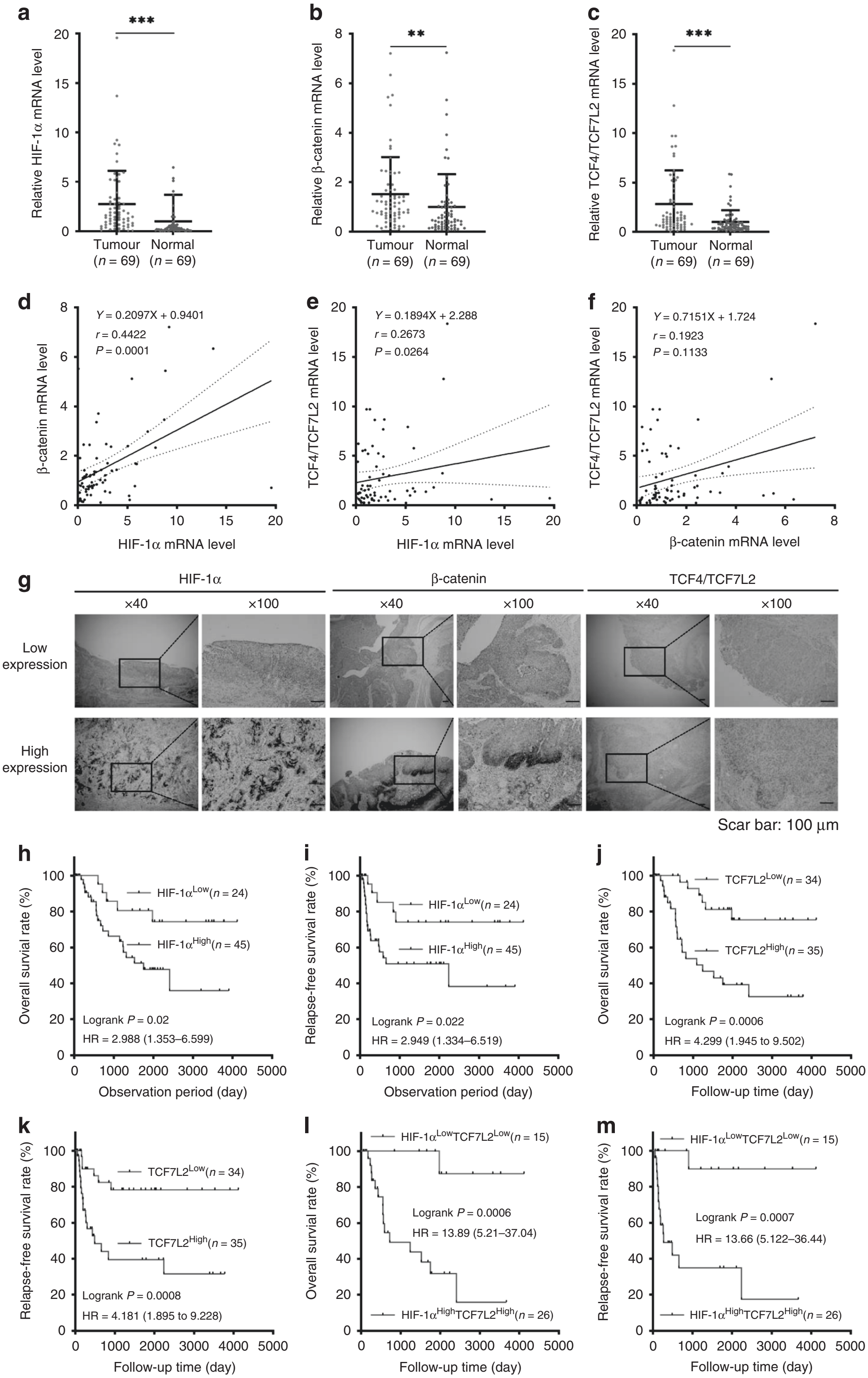

Fig. 6 HIF-1α expression was associated with TCF4/TCF7L2 expression in ESCC tissues, which was correlated with poor prognosis. **a**–**c** HIF-1α, β-catenin and TCF4/TCF7L2 mRNA levels in 69 pairs of neoplastic and matched non-neoplastic oesophageal tissues from ESCC patients. **d**–**f** The relevance of HIF-1α, β-catenin, and TCF4/TCF7L2 mRNA expression levels in tumour tissues in 69 ESCC patients (Spearman's correlation *r* and *P* value are shown). **g** Representative images of immunohistochemistry staining represent the low (upside) and high (downside) protein levels of HIF-1α, β-catenin, and TCF4/TCF7L2 expressed in ESCC tissues. Overall survival (OS) and relapse-free survival (RFS) in ESCC patients with high or low HIF-1α expression (**h**, **i**), high or low TCF4/TCF7L2 expression (**j**, **k**), and the combination of HIF-1α and TCF4/TCF7L2 protein level (**l**, **m**). r Spearman's coefficient, HR hazard ratio. *P* values were determined by log-rank Kaplan–Meier (K–M) analysis.

Table 1. Correlation between HIF-1α expression and clinicopathological characteristics in 69 oesophageal squamous cell carcinoma patients.

	HIF-1α expression level		
	High (45)	**Low (24)**	**P value**[a]
Gender			0.275
Male	37	17	
Female	8	7	
Age (years)			
>68	23	11	0.676
≤68	22	13	
T stage			**0.015**[b]
1	8	13	
2	8	1	
3	26	9	
4	3	1	
N stage			
N0	20	8	**0.023**[b]
N1	8	12	
N2	11	4	
N3	6	0	
Pathological stage			0.321
I	5	7	
II	17	7	
III	17	8	
IV	6	2	
Infiltrative growth (INF)			0.175
a	2	4	
b	41	18	
c	2	2	
Lymphatic invasion			0.280
Positive	23	9	
Negative	22	15	
Vascular invasion			**0.031**[b]
Positive	37	14	
Negative	8	10	
β-catenin expression			**0.003**[b]
High	22	3	
Low	23	21	
TCF4/TCF7L2 expression			0.109
High	26	9	
Low	19	15	

[a] Statistical significance is determined by the Chi-square test or Fisher's exact test.

[b] The bold figures in the table indicate that the P value is statistically significant.

Elevated expression of HIF-1α and TCF4/TCF7L2 predicts poor prognosis of patients with ESCC

To better understand the role of HIF-1α in both clinical characteristics and prognosis, we divided ESCC patients into two groups based on the protein levels of HIF-1α. The results revealed that ESCC patients with elevated HIF-1α expression were statistically significantly associated with T stage ($P = 0.015$), N stage ($P = 0.023$), vascular invasion ($P = 0.031$) and β-catenin expression ($P = 0.003$) (Table 1). Intriguingly, Kaplan–Meier analyses revealed that patients with elevated HIF-1α levels had poorer overall survival (OS) (hazard ratio (HR) = 2.988, $P = 0.02$) (Fig. 6h) and worse relapse-free survival (RFS) (HR = 2.949, $P = 0.022$) (Fig. 6I). Besides, the results further revealed that ESCC patients with high TCF4/TCF7L2 expression had a shorter OS (HR = 4.299, $P = 0.0006$) and RFS (HR = 4.181, $P = 0.0008$) than the low expression group (Fig. 6j, k). There were no differences in OS or RFS between the high and low β-catenin expression groups (Supplementary Fig. 5A, B). Representative images of low (upside) and high (downside) HIF-1α, β-catenin, and TCF4/TCF7L2 staining using IHC analysis are indicated in Fig. 6g.

Recent studies suggest that combining multiple markers may be more effective than a single marker in predicting treatment response and prognosis. Thus, we further divided ESCC patients into four groups based on the combined expression of HIF-1α and TCF4/TCF7L2: HIF-1α^{high} TCF4/TCF7L2^{high}, HIF-1α^{high} TCF4/TCF7L2^{low}, HIF-1α^{low} TCF4/TCF7L2^{high} group and HIF-1α^{low} TCF4/TCF7L2^{low} group. Compared to the HIF-1α^{low} TCF4/TCF7L2^{low} group, ESCC patients in the HIF-1α^{high} TCF4/TCF7L2^{high} group were associated with advanced T stage ($P = 0.019$), N stage ($P = 0.002$), infiltrative growth pattern ($P = 0.007$) and vascular invasion ($P = 0.012$) (Table 2). The ESCC patients in the HIF-1α^{high} TCF4/TCF7L2^{high} group had a poor prognosis (OS, HR = 13.89, $P = 0.0006$; RFS, HR = 13.66, $P = 0.0007$) (Fig. 6l, m), suggesting that the combination of HIF-1α and TCF4/TCF7L2 has a robust prognostic value than either HIF-1α or TCF4/TCF7L2 individually. The OS and RFS analysis of four different groups were present in Supplementary Fig. 5C, D. Ultimately, HIF-1α and TCF4/TCF7L2 were ascertained as independent prognostic factors for ESCC patients based on univariate and multivariate Cox regression analyses (Table 3).

DISCUSSION

The hypoxic microenvironment is one of the most critical features of the solid tumour microenvironment, and it has been shown to be positively correlated with malignancies progression and aggressive phenotype [27]. HIF-1α is the primary regulator of hypoxia-induced cellular biological responses, such as neoangiogenesis, proliferation, and apoptosis resistance [28]. It has recently been depicted that hypoxia not only directly affects tumour cells but also enhances the invasion potential of neoplastic cells by affecting the extracellular matrix, such as cancer-related fibroblasts [29]. Furthermore, hypoxic stress may cause tumour cells to become resistant to multiple therapeutic medications, with the fundamental mechanism possibly being acidification of the extracellular pH (pH_e) and decreased expression of drug flux pump proteins [30]. Overexpression of HIF-1α has been clinically confirmed in a variety of carcinomas, including colorectal [31], breast [32], pancreatic [33], renal [34], ovarian [35] and oesophageal [36]. Consistently, our study demonstrated that HIF-1α is stimulated in ESCC and that elevated HIF-1α is associated with advanced T stage, vascular invasion, and poorer outcomes. More importantly, by establishing physical hypoxia (1% O_2), chemical hypoxia ($CoCl_2$) and HIF-1α-specific loss-of-function models, we further revealed that HIF-1α plays an essential role in hypoxia-induced ESCC progression by maintaining crucial mechanisms such as proliferation, migration/invasion, apoptosis, cell cycle arrest, EMT, and chemoresistance. In conclusion, this work sheds light on the mechanism of HIF-1a in ESCC progression and deepens our comprehension of its role.

Consistent with previous reports [37], in our clinical studies, we discovered that HIF-1α, β-catenin, and TCF4/TCF7L2 were overexpressed in ESCC tissues. Notably, we firstly identified that the combination of HIF-1α and TCF4/TCF7L2 factors has a robust prognostic value in ESCC than using either HIF-1α or TCF4/TCF7L2

Table 2. Correlation between HIF-1α and TCF4/TCF7L2 expression and clinicopathological characteristics in 69 oesophageal squamous cell carcinoma patients.

	HIF-1α/TCF4 expression level		
	HIF-1α^{High}/ TCF4 ^{High} (26)	**HIF-1α^{Low}/ TCF4 ^{Low} (15)**	***P* value**[a]
Gender			0.064
Male	22	8	
Female	4	7	
Age (years)			0.393
>68	12	9	
≤68	14	6	
T stage			**0.019**[b]
1	4	9	
2	2	1	
3	18	5	
4	2	0	
N stage			**0.002**[b]
N0	12	4	
N1	3	10	
N2	8	1	
N3	3	0	
Pathological stage			0.407
I	3	5	
II	9	5	
III	11	4	
IV	3	1	
Infiltrative growth (INF)			**0.007**[b]
a	0	4	
b	25	10	
c	1	1	
Lymphatic invasion			0.837
Positive	13	7	
Negative	13	8	
Vascular invasion			**0.012**[b]
Positive	23	8	
Negative	3	7	

[a] Statistical significance is determined by the Chi-square test or Fisher's exact test.

[b] The bold figures in the table indicate that the *P* value is statistically significant.

individually. Using in vitro systems, we confirmed the oncogenic involvement of HIF-1α in ESCC cells by promoting proliferation, migration/invasion, anti-apoptosis, G0/G1 cell cycle arrest, and EMT activation. Previous studies have reported that $CoCl_2$ promotes cell growth and regulates the cell cycle in the MCF-7 and MDA-MB-231 cell lines by targeting the HIF-1α/VEGF signalling [38]. Herein, $CoCl_2$ remarkably stimulated ESCC cells proliferation while inhibiting apoptosis. However, it is key to note that our research revealed that hypoxia (1% O_2) inhibited ESCC cells proliferation. There are several possible reasons for the unexpected responses. $CoCl_2$ affects the transcription of different genomes that are not subjected to physically induced hypoxia, suggesting that the genes induced by these two hypoxia models do not completely overlap [39]. However, it has been observed that the metabolic responses of cells differ in physical hypoxia and chemically induced hypoxia by $CoCl_2$ [40]. In a nutshell, the physical and chemical hypoxia models are largely consistent in their effects on the malignant progression of ESCC, and this may provide clues for subsequent future studies on the field of hypoxia in ESCC.

The most accepted explanation for EMT and metastasis is that cancer progenitor cells may undergo EMT in order to differentiate further [41]. Research indicates that in hepatocellular carcinoma cells, HIF-1α promotes cell migration, invasion, and activation of EMT via the $Ca2^{+}$/PI3K/AKT signalling [42]. It is well known that downregulation of E-cadherin expression supports cancer cell migration and metastasis, and we demonstrate a critical role for HIF-1α in hypoxia-mediated transcriptional and translational repression of E-cadherin. In addition, this study also firstly revealed the crucial role of HIF-1α in hypoxia (1% O_2 and $CoCl_2$) induced 5-fluorouracil (5-FU) resistance in ESCC cell lines. Emerging evidence suggests that hypoxia contributes to chemoresistance in ESCC during the administration of first-line drugs, such as Cisplatin and 5-fluorouracil (5-FU) [43]. The involvement of HIF-1α in 5-fluorouracil (5-FU) resistance in ESCC was further confirmed using in vivo experiments. Another widely recognised mechanism that is regulated by hypoxia and responsible for cancer progression is angiogenesis. We observed a significant decrease in tumour growth inhibition in the 5-fluorouracil (5-FU) combined with the HIF-1α-shRNA treatment group of nude mice, accompanied by a reduction in the counts of neovascularization microvessels. Therefore, it is worth noting that the strategy of combining 5-fluorouracil(5-FU) with HIF-1α targeted inhibition may provide a more practical approach for those 5-fluorouracil(5-FU)-resistant clinical patients in the future.

The Wnt oncogenic signalling pathway is characterised by the activation of β-catenin and downstream effectors LEF/TCF transactivation. β-catenin is generally considered an essential member of the cadherin complexes, which interacts with E-cadherin to form a heterodimer, regulates cell-to-cell adhesion, and further affects cell migration and invasion [44]. Previously, it was shown that the complex crosstalk between HIF-1α and Wnt/β-catenin signalling in hepatocellular carcinoma, as well as the HIF-1α/β-catenin complex, enhances β-catenin transcription activities [45], consistent with this, we also observed the presence of the HIF-1α/β-catenin complex in ESCC cells. TCF4/TCF7L2 is a critical effector of canonical Wnt signalling, activating β-catenin/TCF target genes such as c-myc [46] and cyclin D1 [47], and resulting in specific cellular responses [48]. A previous study reported the expression of TCF4/TCF7L2 in human oesophageal cancer tissues and cell lines and further demonstrated that TCF4/TCF7L2 promotes the proliferation of EC109 cells [49]. In addition, TCF4/TCF7L2 is predominantly expressed in the nucleus of oesophageal cancer cells, and elevated TCF4/TCF7L2 is associated with advanced T stage and worse outcomes in ESCC [37]. In this work, HIF-1α mediated TCF4/TCF7L2 transcriptional activities by directly associating with the promoter of TCF4/TCF7L2, given the specific binding of β-catenin to TCF4/TCF7L2, it is reasonable to speculate that the binding of HIF-1α to TCF4/TCF7L2 is guided by β-catenin. Thus, more experiments are needed to clarify the specific pattern of TCF4/TCF7L2 occupied by the HIF-1-α protein.

CONCLUSION

In summary, we observe that HIF-1-α promotes ESCC progression by activating Wnt/β-catenin signalling via targeting the TCF4/TCF7L2 promoter region and transactivation of TCF4/TCF7L2. Our findings indicate that combinations targeting HIF-1α and Wnt/β-catenin signalling deserve more attention to achieve a better therapeutic effect in ESCC.

Table 3. Univariate and multivariate Cox regression analysis.

Clinical features	Univariate analysis			Multivariate analysis		
	HR	95% CI	*P* value	HR	95% CI	*P* value
Gender	0.249	0.059–1.056	0.059			
Age (years)	1.018	0.962–1.076	0.541			
T stage	2.227	0.833–5.948	0.110			
N stage	3.330	1.246–8.896	**0.016**[a]	6.384	1.943–20.973	**0.002**[a]
Pathological stage	7.104	0.959–52.635	0.055			
Infiltrative growth	1.200	0.283–5.092	0.805			
Lymphatic invasion	2.087	0.936–4.651	0.072			
Vascular invasion	4.227	1.259–14.192	**0.020**[a]	1.436	0.353–5.847	0.613
HIF-1α expression	3.059	1.137–8.231	**0.027**[a]	4.252	1.451–12.457	**0.008**[a]
β-catenin expression	1.538	0.688–3.440	0.294			
TCF4 expression	4.362	1.736–10.958	**0.002**[a]	6.317	2.408–16.572	**0.000**[a]

[a] The bold figures in the table indicate that the *P* value is statistically significant.

DATA AVAILABILITY

All data required to evaluate the findings in the paper is available in the paper and supplementary materials.

REFERENCES

1. Pennathur A, Gibson MK, Jobe BA, Luketich JD. Oesophageal carcinoma. Lancet. 2013;381:400–12.
2. Lagergren J, Smyth E, Cunningham D, Lagergren P. Oesophageal cancer. Lancet. 2017;390:2383–96.
3. Wilson WR, Hay MP. Targeting hypoxia in cancer therapy. Nat Rev Cancer. 2011;11:393–410.
4. Ke Q, Costa M. Hypoxia-inducible factor-1 (HIF-1). Pharmacol. 2006;70:1469–80.
5. Hajizadeh F, Okoye I, Esmaily M, Ghasemi Chaleshtari M, Masjedi A, Azizi G, et al. Hypoxia inducible factors in the tumor microenvironment as therapeutic targets of cancer stem cells. Life Sci. 2019; https://doi.org/10.1016/j.lfs.2019.116952.
6. Heddleston JM, Li Z, Lathia JD, Bao S, Hjelmeland AB, Rich JN. Hypoxia inducible factors in cancer stem cells. Br J Cancer. 2010; https://doi.org/10.1038/sj.bjc.6605551.
7. Wiesener MS, Jürgensen JS, Rosenberger C, Scholze CK, Hörstrup JH, Warnecke C, et al. Widespread hypoxia-inducible expression of HIF-2alpha in distinct cell populations of different organs. FASEB J. 2003. https://doi.org/10.1096/fj.02-0445fje.
8. Keith B, Simon MC. Hypoxia-inducible factors, stem cells, and cancer. Cell. 2007;129:465–72.
9. Gonzalez FJ, Xie C, Jiang C. The role of hypoxia-inducible factors in metabolic diseases. Nat Rev Endocrinol. 2018;15:21–32.
10. Eubank TD, Roda JM, Liu H, O'Neil T, Marsh CB. Opposing roles for HIF-1α and HIF-2α in the regulation of angiogenesis by mononuclear phagocytes. Blood. 2011. https://doi.org/10.1182/blood-2010-01-261792.
11. Zhang Y, Wang X. Targeting the Wnt/β-catenin signaling pathway in cancer. J Hematol Oncol. 2020;13:165.
12. Boso D, Rampazzo E, Zanon C, Bresolin S, Maule F, Porcù E, et al. HIF-1α/Wnt signaling-dependent control of gene transcription regulates neuronal differentiation of glioblastoma stem cells. Theranostics. 2019;9:4860–77.
13. Jiang N, Zou C, Zhu Y, Luo Y, Chen L, et al. HIF-1α-regulated miR-1275 maintains stem cell-like phenotypes and promotes the progression of LUAD by simultaneously activating Wnt/β-catenin and Notch signaling. Theranostics. 2020;10:2553–70.
14. Scholten DJ 2nd, Timmer CM, Peacock JD, Pelle DW, Williams BO, Steensma MR. Down regulation of Wnt signaling mitigates hypoxia-induced chemoresistance in human osteosarcoma cells. PLoS ONE. 2014;9:e111431.
15. Sashiyama H, Shino Y, Kawamata Y, Tomita Y, Ogawa N, Shimada H, et al. Immortalization of human esophageal keratinocytes by E6 and E7 of human papillomavirus type 16. Int J Oncol. 2001;19:97–103.
16. Ji Z, Yang G, Shahzidi S, Tkacz-Stachowska K, Suo Z, Nesland JM. Induction of hypoxia-inducible factor-1alpha overexpression by cobalt chloride enhances cellular resistance to photodynamic therapy. Cancer Lett. 2006. https://doi.org/10.1016/j.canlet.2005.12.010.
17. Dai M, Cui P, Yu M, Han J, Li H, Xiu R. Melatonin modulates the expression of VEGF and HIF-1 alpha induced by $CoCl_2$ in cultured cancer cells. J Pineal Res. 2008;44:121–6.
18. Toyozumi T, Hoshino I, Takahashi M, Usui A, Akutsu Y, Hanari N, et al. Fra-1 Regulates the expression of HMGA1, which is associated with a poor prognosis in human esophageal squamous cell carcinoma. Ann Surg Oncol. 2017. https://doi.org/10.1245/s10434-016-5666-5.
19. Livak KJ, Schmittgen TD. Analysis of relative gene expression data using real-time quantitative PCR and the 2(-Delta Delta C(T)) method. Methods. 2001;25:402–8.
20. Liu DS, Read M, Cullinane C, Azar WJ, Fennell CM, Montgomery KG, et al. APR-246 potently inhibits tumour growth and overcomes chemoresistance in preclinical models of oesophageal adenocarcinoma. Gut. 2015;64:1506–16.
21. Weidner N, Semple JP, Welch WR, Folkman J. Tumor angiogenesis and metastasis-correlation in invasive breast carcinoma. N Engl J Med. 1991;324:1–8.
22. Pastushenko I, Blanpain C. EMT transition states during tumor progression and metastasis. Trends Cell Biol. 2019; https://doi.org/10.1016/j.tcb.2018.12.001.
23. Mazumdar J, O'Brien WT, Johnson RS, LaManna JC, Chavez JC, Klein PS, et al. O_2 regulates stem cells through Wnt/β-catenin signalling. Nat Cell Biol. 2010;12:1007–13.
24. Liu HL, Liu D, Ding GR, Liao PF, Zhang JW. Hypoxia-inducible factor-1α and Wnt/β-catenin signaling pathways promote the invasion of hypoxic gastric cancer cells. Mol Med Rep. 2015; https://doi.org/10.3892/mmr.2015.3812.
25. Hong CF, Chen WY, Wu CW. Upregulation of Wnt signaling under hypoxia promotes lung cancer progression. Oncol Rep. 2017; https://doi.org/10.3892/or.2017.5807.
26. Xu W, Zhou W, Cheng M, Wang J, Liu Z, He S, et al. Hypoxia activates Wnt/β-catenin signaling by regulating the expression of BCL9 in human hepatocellular carcinoma. Sci Rep. 2017. https://doi.org/10.1038/srep40446
27. Muz B, de la Puente P, Azab F, Azab AK. The role of hypoxia in cancer progression, angiogenesis, metastasis, and resistance to therapy. Hypoxia. 2015;3:83–92.
28. Pouysségur J, Dayan F, Mazure NM. Hypoxia signalling in cancer and approaches to enforce tumour regression. Nature. 2006;441:437–43.
29. Jing X, Yang F, Shao C, Wei K, Xie M, Shen H. Role of hypoxia in cancer therapy by regulating the tumor microenvironment. Mol Cancer. 2019;18:157.
30. Belisario DC, Kopecka J, Pasino M, Akman M, De Smaele E, Donadelli M. Hypoxia dictates metabolic rewiring of tumors: implications for chemoresistance. Cells. 2020;9:2598.
31. Kaidi A, Williams AC, Paraskeva C. Interaction between beta-catenin and HIF-1 promotes cellular adaptation to hypoxia. Nat Cell Biol. 2007; https://doi.org/10.1038/ncb1534.
32. Rezaeian AH, Li CF, Wu CY, Zhang X, Delacerda J, You MJ, et al. A hypoxia-responsive TRAF6-ATM-H2AX signalling axis promotes HIF1α activation, tumorigenesis and metastasis. Nat Cell Biol. 2017; https://doi.org/10.1038/ncb3445.
33. Liu M, Zhong J, Zeng Z, Huang K, Ye Z, Deng S, et al. Hypoxia-induced feedback of HIF-1α and lncRNA-CF129 contributes to pancreatic cancer progression through stabilization of p53 protein. Theranostics. 2019;9:4795–810.
34. Alsaab HO, Sau S, Alzhrani RM, Cheriyan VT, Polin LA, Vaishampayan U. Tumor hypoxia directed multimodal nanotherapy for overcoming drug resistance in renal cell carcinoma and reprogramming macrophages. Biomaterials. 2018; https://doi.org/10.1016/j.biomaterials.2018.08.053.
35. Kitajima S, Lee KL, Hikasa H, Sun W, Huang RY, Yang H, et al. Hypoxia-inducible factor-1α promotes cell survival during ammonia stress response in ovarian cancer stem-like cells. Oncotarget. 2017;8:114481–94.
36. Koukourakis MI, Giatromanolaki A, Skarlatos J, Corti L, Blandamura S, Piazza, et al. Hypoxia inducible factor (HIF-1a and HIF-2a) expression in early esophageal

cancer and response to photodynamic therapy and radiotherapy. Cancer Res. 2001;61:1830–2.

37. Ishiguro H, Wakasugi T, Terashita Y, Sakamoto N, Tanaka T, Sagawa H, et al. Nuclear expression of TCF4/TCF7L2 is correlated with poor prognosis in patients with esophageal squamous cell carcinoma. Cell Mol Biol Lett. 2016;21:5.
38. Rana NK, Singh P, Koch B. CoCl2 simulated hypoxia induce cell proliferation and alter the expression pattern of hypoxia associated genes involved in angiogenesis and apoptosis. Biol Res. 2019;52:12.
39. Vengellur A, Phillips JM, Hogenesch JB, LaPres JJ. Gene expression profiling of hypoxia signaling in human hepatocellular carcinoma cells. Physiol Genomics. 2005; https://doi.org/10.1152/physiolgenomics.00045.2004.
40. Borcar A, Menze MA, Toner M, Hand SC. Metabolic preconditioning of mammalian cells: mimetic agents for hypoxia lack fidelity in promoting phosphorylation of pyruvate dehydrogenase. Cell Tissue Res. 2013; https://doi.org/10.1007/s00441-012-1517-2.
41. Heerboth S, Housman G, Leary M, Longacre M, Byler S, Lapinska K, et al. EMT and tumor metastasis. Clin Transl Med. 2015;4:6.
42. Dou C, Zhou Z, Xu Q, Liu Z, Zeng Y, Wang Y, et al. Hypoxia-induced TUFT1 promotes the growth and metastasis of hepatocellular carcinoma by activating the Ca2+/PI3K/AKT pathway. Oncogene. 2019; https://doi.org/10.1038/s41388-018-0505-8.
43. Luan S, Zeng X, Zhang C, Qiu J, Yang Y, Mao C, et al. Advances in drug resistance of esophageal cancer: from the perspective of tumor microenvironment. Front Cell Dev Biol. 2021;9:664816.
44. Wu ZQ, Li XY, Hu CY, Ford M, Kleer CG, Weiss SJ. Canonical Wnt signaling regulates Slug activity and links epithelial-mesenchymal transition with epigenetic breast cancer 1, early onset (BRCA1) repression. Proc Natl Acad Sci USA. 2012; https://doi.org/10.1073/pnas.1205822109.
45. Zhang Q, Bai X, Chen W, Ma T, Hu Q, Liang C, et al. Wnt/β-catenin signaling enhances hypoxia-induced epithelial-mesenchymal transition in hepatocellular carcinoma via crosstalk with hif-1α signaling. Carcinogenesis. 2013; https://doi.org/10.1093/carcin/bgt027.
46. He TC, Sparks AB, Rago C, Hermeking H, Zawel L, da Costa LT, et al. Identification of c-MYC as a target of the APC pathway. Science. 1998;281:1509–12.
47. Ju X, Casimiro MC, Gormley M, Meng H, Jiao X, Katiyar S, et al. Identification of a cyclin D1 network in prostate cancer that antagonizes epithelial-mesenchymal restraint. Cancer Res. 2014; https://doi.org/10.1158/0008-5472.CAN-13-1313.
48. Nusse R, Clevers H. Wnt/β-catenin signaling, disease, and emerging therapeutic modalities. Cell. 2017;169:985–99.
49. He G, Guan X, Chen X, Wang Y, Luo C, Zhang B. Expression and splice variant analysis of human TCF4 transcription factor in esophageal cancer. J Cancer. 2015;6:333–41.

ACKNOWLEDGEMENTS

We sincerely thank the first author's wife, Dr. Xiayun Wan, for her psychological counselling during the author's writing period.

AUTHOR CONTRIBUTIONS

KT, TT, KM, HS, MK, SE, YM, MU, KH and HM conceived this study. KT performed all the experiments. HS, MT, NS, RO, KK, SH and JH monitored the progress of the experiment, provided comments and helped write the manuscript. KT performed the statistics and wrote the manuscript. TT revised the manuscript. HM approved the final version. All authors have reviewed the manuscript and all have approved the submission.

FUNDING

Not applicable.

COMPETING INTERESTS

The authors declare no competing interests.

ETHICS APPROVAL AND CONSENT TO PARTICIPATE

This research was performed in accordance with the Declaration of Helsinki. Our animal research was approved by the Animal Care and Use Committee of Chiba University (No. A3-22) and follows the policies for institutional animal care. The clinical analyses in this study were authorised by the Institutional Review Board of Chiba University (No. 1120-942) and written informed consent was obtained from all participants.

CONSENT TO PUBLISH

All authors have reviewed the final version of the manuscript and consent to its publication.

ADDITIONAL INFORMATION

Supplementary information The online version contains supplementary material available at https://doi.org/10.1038/s41416-022-01825-3.

Correspondence and requests for materials should be addressed to Takeshi Toyozumi.

Reprints and permission information is available at http://www.nature.com/reprints

Publisher's note Springer Nature remains neutral with regard to jurisdictional claims in published maps and institutional affiliations.